Automatic generation control of multi area thermal system using Bat algorithm optimized PDâ€"PID cascade controller

kothai M
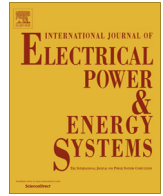
Need to cite this paper?

Get the citation in MLA, APA, or Chicago styles

Want more papers like this?

Download a PDF Pack of related papers

Search Academia's catalog of 22 million free papers

Automatic generation control of multi area thermal system using Bat algorithm optimized PD–PID cascade controller

Puja Dash *, Lalit Chandra Saikia [1], Nidul Sinha

Department of Electrical Engineering, National Institute of Technology Silchar, Assam, India

A B S T R A C T

This article presents automatic generation control (AGC) of an interconnected multi area thermal system. The control areas are provided with single reheat turbine and generation rate constraints of 3%/min. A maiden attempt has been made to apply a Proportional derivative–Proportional integral derivative (PD–PID) cascade controller in AGC. Controller gains are optimized simultaneously using more recent and powerful evolutionary computational technique Bat algorithm (BA). Performance of classical controllers such as Proportional Integral (PI) and Proportional Integral Derivative (PID) controller are investigated and compared with PD–PID cascade controller. Investigations reveal that PI, and PID provide more or less same response where as PD–PID cascade controller provides much better response than the later. Dynamic analysis has also been carried out for the controllers in presence of random load pattern, which reveals the superior performance of the PD–PID cascade controller. Sensitivity analysis reveals that the BA optimized PD–PID Cascade controller parameters obtained at nominal condition of loading, size and position of disturbance and system parameter (Inertia constant, H) are robust and need not be reset with wide changes in system loading, size, position of disturbance and system parameters. The system dynamic performances are studied with 1% step load perturbation in Area1.

© 2015 Elsevier Ltd. All rights reserved.

Introduction

In automatic generation control (AGC) of interconnected power system puts the limelight towards the maintenance of system frequency within specified limits around the nominal value, to uphold the scheduled exchange of power between the interconnected areas and to keep each unit's generation at the most economic level. This requires the balance between the net generation and corresponding loads with losses. Many investigative research works exist in the past literature on AGC of isolated and interconnected systems. The idea of modeling multi-area interconnected power system has been presented by Elgerd and Fosha [1]. A performance comparison of several classical controllers, such as Integral (I), Proportional-Integral (PI), Integral-Derivative (ID), Proportional-Integral-Derivative (PID) and Integral-Double Derivative (IDD) have been carried out by Saikia et al. [2]. Their investigations reveal the superior performance of IDD controller in two, three and five area thermal systems. However, their studies are limited to single controllers where there is less number of tuning

knob. If tuning knobs are more in a controller, there may be possibility of better result from that controller. A two degree of freedom (2DOF) controller named as 2DOF-PID has been introduced by Sahu et al. [3] in AGC. Later on, the performance of a new 2DOF controller named as 2DOF- Integral double derivative (2DOF-IDD) has been evaluated by Puja Dash et al. [4]. However, all the above controllers are non cascaded single controllers. In process control, many controllers and control strategies are available. These are suitable for controlling large-scale networked systems. In the controlling process, the controllers are either optimized by optimization techniques or self tuned with the help of different control strategies such as model predictive control (MPC), Smith predictor, etc. Yongho Lee et al. [5] proposed a method for PID controller tuning based on process models for cascaded control systems. Cheng et al. [6] have made application of two PID controllers in a cascade control system directly based on the process data collected from a one-shot plant and found it to be the best. Rather than cascade control, many other control approaches generally model based controls are commonly used in process control such as Neural network control [7], fuzzy based control [8], MPC [9,10], Smith predictor [13], etc. Saikia [7] has applied the multi layer perception neural network (MLPNN) controller using reinforcement learning in AGC of a three area thermal system. Chown and Hartman [8] has implemented the fuzzy controller in the control ACE (area con-

Nomenclature

n	population size	T_{pi}	$2H_i/f^* D_i$
N	number of generations	K_{pi}	$1/D_i$. (Hz/pu)
a	loudness	K_{Ii}	integral gain of PI, PID controller in area i
r	pulse rate	K_{Di}	derivative gain of PI, PID controller in area i
f	nominal system frequency (Hz)	K_{Pi}	proportional gain of PI, PID controller in area i
i	subscript referred to area i (1, 2, 3)	K_{Iij}	integral gain of PID controller in area i, for $i = 1, j = 2$ (for $i \neq j$), 3)
$*$	superscript denotes optimum value		
P_{ri}	rated power of area i (MW)	K_{Pij}	integral gain of PID controller in area i, for $i = 1, j = 2$ (for $i \neq j$), 3)
H_i	inertia constant of area i (s)		
ΔP_{Di}	incremental load change in area i (p.u)	K_{Dij}	integral gain of PID controller in area i, for $i = 1, j = 2$ (for $i \neq j$), 3)
ΔP_{gi}	Incremental generation change in area i (p.u)		
D_i	$\Delta P_{Di}/\Delta f_i$(pu/Hz)	β_i	(=$D_i + 1/R_i$), Area frequency response characteristics of area (AFRC) i
T_{12}, T_{23}, T_{13}	synchronizing coefficients		
R_i	governor speed regulation parameter of area i (Hz/pu MW)	J	cost index ($J = \int_0^T \{(\Delta f_i)^2 + (\Delta P_{tie j-k})^2\}dt$), $j = 1, 2, k = 2$ (for $k \neq j$), 3)
T_{gi}	steam governor time constant of area i (s)	T	simulation time (s)
K_{ri}	steam turbine reheat coefficient of area i	Δf_i	incremental change in frequency of area i (Hz)
T_{ri}	steam turbine reheat time constant of area i (s)	ΔP_{gi}	Incremental generation of area i (p.u);
T_{ti}	steam turbine time constant of area i (s)	$\Delta P_{tie\ i-j}$	incremental change in tie line power connecting between area i and area j (p.u)
B_i	frequency bias constant of area i		

trol error) calculation in AGC, which determines the shortfall or surplus generation that has to be corrected. MPC is a family of controllers in which there is a direct uses of an explicit certain model. It is also described as a class of computer control schemes that utilizes a process model [9,10]. In AGC, the MPC control technique has been applied successfully [11,12] to accomplish the desired control of frequency automatically. Venkat et al. [11] have designed a distributed model predictive control (MPC) framework for controlling of large-scale networked systems such as AGC of power systems. Liu et al. [12] has employed MPC to control load frequency of a non-reheat type two area thermal systems. The Smith predictor, another popular control in process industry is available in literature [13]. Smith predictor with cascade controller has been used in controlling the temperature of a gas furnace. As these model based controls have many advantages, also having some limitations such as (a) Modeling of error can essentially influence the performance of the controller, during the tuning of the controller the robustness properties of the resulted control loop must be considered, (b) Its derivation is more complex than the traditional PID controller. [9]. However, the advantages of these model based control processes dominate the limitations. Many research works are present in process control industry, where the performance of cascade controller is improved by incorporating with model predictive control [12], Smith predictor control techniques [13]. This review of literatures gives the limelight towards the heuristically optimized cascade controller which is simple to apply and is not yet investigated in AGC. Hence, this necessitates further investigation.

Many control and optimization, such as classical, optimal, fuzzy logic (FL), artificial neural networks (ANN), genetic algorithm, bacterial forging, particle swarm, DE, firefly algorithms (FA) are available and most of them are used in AGC. Classical technique is a trial and error method and in some cases yields suboptimal results and time consuming [14]. Some literatures exist about the application of supervised artificial neural networks [7,15] and some authors have used fuzzy logic (FL) controller [8,16] for achieving better performance in AGC. In case of FL controller, more computational time is required for rule base to be formed. In case of neural network, time required for training is more. Modern metaheuristic algorithms have been developed with an aim to carry out inclusive search, which cannot be solved by classical techniques. The efficiency of metaheuristic algorithms can be ascribed to the fact that

they imitate the best features in nature, especially the selection of the fittest in biological systems, which have evolved by natural selection over millions of years. As given the features or nature of a particular problem, one type of search algorithm may prove to be more efficient than others in solving that particular problem, while the same algorithm may perform poorly in other problems. GA has been applied for optimization of controller gains [16] and recent research identified some of the deficiencies. To overcome the difficulties of local optimum methods, BF [17] technique is used by the researcher for optimization. In [17] the foraging behavior of bacteria is formulated as an optimization technique. Another metaheuristic algorithm, fire fly algorithm (FA) is developed by [18] and successfully applied in AGC of an isolated CCGT plant [19]. A more recent meta-heuristic search algorithm, Cuckoo search (CS) has been developed by Yang and Deb [20]. Cuckoo is a fascinating bird, for its beautiful sounds they can make and for their aggressive reproduction strategy. Ani and Guira, species of cuckoos lay their eggs in communal nests, though they may remove others' eggs to increase the hatching probability of their own eggs [21]. Quite a number of species engage the obligate brood parasitism by laying their eggs in the nests of other host birds (often other species). CS algorithm is based on the obligate brood parasitic behavior of some cuckoo species in combination with the Lévy flight behavior. The cuckoo's follow three basic types of brood parasitism such as Intraspecific brood parasitism, Cooperative breeding, and Nest takeover. CS algorithm follows three idealized rules. They are (a) Each cuckoo lays one egg at a time, and dumps it in a randomly chosen nest, (b) The best nests with high quality of eggs (solutions) will carry over to the next generations, (c) The number of available host nests is fixed, and a host can discover an alien egg with a probability pa $\in$ [0,1]. This powerful algorithm has been proved its fast and accurate optimization proficiency in various relevance grounds [21]. Tan et al. [22] used the CS algorithm for allocation and sizing of DG. Yildiz [23] has tested this CS algorithm for the selection of optimal machining parameters in milling operations, and has got a superior conclusion, where Bhandari et al. has applied the CS algorithm for satellite image contrast and brightness enhancement using [24]. Dash et al. [4,25] used CS for optimization of 2DOF-IDD controller gains in multi area thermal systems. Nguyen et al. [26] used the CS algorithm for solving short-term hydrothermal scheduling problem. A

new simple and powerful metaheuristic population based algorithm, named as Bat Algorithm (BA) is also found in the literature [27]. BA is based on the echolocation behavior of Bats, which combines local search through random walks and global exploration. A poor balance between exploration and exploitation may result in a weak optimization method, which may suffer from premature convergence, trapping in a local optima and stagnation. BA is reported to be so efficient and successful among the population based algorithms due to some of the features, such as frequency tuning, automatic zooming, and parameter control [27–32]. Sensitivity analysis has been carried out to see the robustness of the optimum parameters for the best controllers [4,17]. The authors have carried out sensitivity analysis for the best classical controller parameters on the basis of dynamic study. However, the same is not done on the basis of dynamic analysis of the system based on the controller gains. This requires further studies. In view of above brief literature study, following are the main objectives of the present work.

(a) Optimization of controller gains of several controllers such as PD–PID Cascade, PI and PID controller, when these controllers are considered separately in a three area thermal system using BA.
(b) Comparison of dynamic responses for evaluation of dynamic performances for PD–PID Cascade controller, PI and PID controllers to find the best.
(c) Comparison of dynamic responses for evaluation of dynamic performances for PD–PID Cascade controller and PID controllers with random load pattern to check the robustness of the proposed controller.
(d) Sensitivity analysis of the optimum parameters of the best controller obtained from (a) at nominal conditions.

System investigated

The system considered is a three unequal area thermal system of capacities Area1: 2000 MW, Area2: 6000 MW, and Area3: 12,000 MW. The areas are equipped with single reheat turbine

and generation rate constraints (GRC) of 3%/min. The nominal system parameters are taken from [2] and are shown in Appendix A. Per unit values of various parameters of the unequal areas are considered to be the same on their respective bases. Hence, in the modeling the interconnected three area system the quantities $a_{12} = -P_{r1}/P_{r2}$, $a_{23} = -P_{r2}/P_{r3}$, $a_{13} = -P_{r1}/P_{r3}$ are taken. Controllers such as PI, PID and PD–PID cascade controllers are considered as separately in this system. The system dynamic performance has been evaluated considering 1% step load perturbation (SLP) in area1. The transfer model of the system is shown in Fig. 1. Matlab software has been used for simulink model and coding. The variables such as controller gains etc are optimized using Bat algorithm (BA). The optimization is done using minimization of the cost function given by Integral squared error (ISE) as given by Eq. (1)

$$J = \int_0^T \{(\Delta f_i)^2 + (\Delta P_{tie\,j-k})^2\}dt \tag{1}$$

where j = area number (1, 2), k = 2 (for $j \neq k$), 3.

PD–PID Cascade controller

Cascade control concept comes up from the control of two sequential processes, where the inner process or output of the first supplies the second or outer process in sequence. There is the measurement is available for both the output of the inner process and outer process variable. The main objectives of cascade control [33]:

(a) The inner measure to attenuate the effect of supply disturbance or any internal process disturbance on the outer process in the sequence.
(b) The outer process measurement to control the process final output quality.

The Cascade control is mainly used to achieve fast rejection of disturbance before it propagates to the other parts of the plant

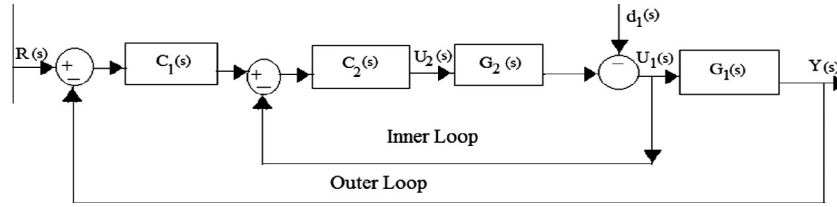**Fig. 1.** Transfer function model of the system with cascade controllers.
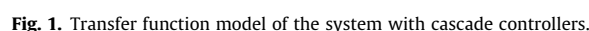
Fig. 2. PD–PID Cascade Controller model.

[5,6,33,34]. The simplest cascade control system involves two control loops (inner and outer) as shown in Fig. 2.

Outer loop

The outer loop is generally referred as the master or primary loop. It contains the process output $Y(s)$, which is under primary control. The outer process is termed as $G_1(s)$ and the whole process is subjected to load disturbance d_1 (s) [33]. The outer loop equation [5] is given as

$$Y(s) = G_1(s)U_1(s) + d_1(s) \qquad (2)$$

where the outer process input is $U_1(s) = y_2(s)$, so that the output from the inner process $y_2(s)$ becomes the input $U_1(s)$ to the outer process. The outer process output is to be controlled to attain a given reference signal $R(s)$ [5,33].

Inner loop

The inner loop is referred as the secondary or slave loop. The loop contains the inner or supply process $G_2(s)$ [33]. The inner loop equation is given as

$$y_2(s) = G_2(s)U_2(s) \qquad (3)$$

where $U_2(s)$ = the inner process input. The output from the inner process becomes the input to the outer process $U_1(s) = y_2(s)$. The control of the inner process uses the inner loop and this comprises an inner comparator and an inner loop measurement of output $y_2(s)$. The main objective of the inner loop is to limit the effect of inner process gain variations on the control system performance [5,33]. Such gain variations might arise from changes in operating point due to set point changes or sustained disturbances. The advantages of cascade controller as compared to other single loop controllers [9,33] are (a) Disturbances arising in the inner loop are corrected by the inner controller before they influence the outer loop controller variable. The correction is much better when the inner loop has a faster response than the outer loop; (b) The speed of system response is greatly improved if the resulting inner control loop has a faster response than the outer loop process; (c) Because of the auxiliary feedback, parameters variations in the inner loop process can be corrected within its own loop.

In this paper, the system is designed with a single loop control system with a PD controller and a cascade control system with a PID controller. The responses of the two control systems are compared for both reference tracking and disturbance rejection. Two controllers are selected and termed here as $C_1(s)$ and $C_2(s)$ as the outer controller and the inner controller respectively. Here, PD controller is made as outer controller and PID as inner controller and are represented as

$$C_1(s) = K_p + K_d s \qquad (4)$$

$$C_2(s) = K_p + \frac{K_i}{s} + K_d s \qquad (5)$$

The overall performance of the cascade system can be analyzed with the decomposed performance diagram as shown in Fig. 2 and the closed loop transfer function [33] can be represented as

$$Y(s) = \left[\frac{G_1(s)G_2(s)C_1(s)C_2(s)}{1 + G_2(s)C_2(s) + G_1(s)G_2(s)C_1(s)C_2(s)} \right] R(s)$$
$$+ \left[\frac{G_1(s)}{1 + G_2(s)C_2(s) + G_1(s)G_2(s)C_1(s)C_2(s)} \right] d_1(s) \qquad (6)$$

Here, in the AGC loop of the reheat type thermal system, $G_1(s)$ = Primary Control loop; $G_2(s)$ = Secondary Control loop; and $d_1(s)$ = load disturbance (SLP). For design of the PD–PID Cascade controller for the investigated system a more recent and powerful algorithm "Bat Algorithm (BA)" is used. The gains of primary and secondary controllers such as K_{Pi}, K_{Di}, and K_{Ii} are optimized simultaneously. The design problem can be formulated as the following constrained optimization problem, where the constraints are the PD–PID Cascade controller parameter bounds given below:

Minimize the objective function = J, Eq. (1).

Subject to $K_{Pi}^{min} \le K_{Pi} \le K_{Pi}^{max}$; $K_{Ii}^{min} \le K_{Ii} \le K_{Ii}^{max}$; $K_{Di}^{min} \le K_{Di} \le K_{Di}^{max}$ (7)

where $K_{Pi}^{min}, K_{Pi}^{max}, K_{Ii}^{min}, K_{Ii}^{max}, K_{Di}^{min}, K_{Di}^{max}$ are the minimum values and maximum values of controller gains respectively. The minimum and maximum bounds for controller gains are chosen as 0 and 1.

Bat Algorithm (BA)

Bat Algorithm is a meta-heuristic nature inspired algorithm for the first time developed by Yang [30]. Among all bats, microbats use echolocation to distinguish their prey, avoid obstacles, and identify their roosting crevices in the dark. Microbats can also use time delay between their ears and loudness variations to sense three-dimensional surroundings. Mainly some features of the echolocation are chosen in optimization problem so that they can be linked with the objective function, which makes it possible to formulate a smart, bat algorithm. They emit loud sound and hear back the echo that comes from nearby objects. The sound pulse they use varies with their hunting strategies. Studies show that microbats emit sound waves with frequency in the range of 20–150 kHz. They also have good sight and hearing capabilities. To determine the location and size of their prey, they rely on the frequency of the echo reaching to their ears. The BA is formulated idealizing bats characteristics in hunting their prey. The bat algorithm is formulated by idealizing the echolocation behavior of bats at first, which includes the behavior of microbats and Acoustics of Echolocation [29,30]. For simplicity, the following approximate or idealized rules are generally followed. (a) All bats use echolocation to sense distance, and they also 'know' the difference between food/prey and background barriers in some magical way. (b) Bats fly randomly with velocity v_i at position x_i with a fixed frequency f_{min}, varying wavelength λ and loudness A_0 to search for prey. They can automatically adjust the wavelength (or frequency) of their emitted pulses and adjust the rate of pulse emission $r \in [0, 1]$, depending on the proximity of their target. (c) As the speed of sound in air is typically v = 340 m/s, the wavelength λ of the ultrasonic sound bursts with a constant frequency is given by (4). (d) Although the loudness can vary in many ways, it can be assumed

that the loudness varies from a large (positive) A_0 to a minimum constant value A_{min}.

$$f = \frac{v}{\lambda} \tag{8}$$

Bat motion

Each bat is associated with a velocity v_i^t and a location x_i^t, at iteration t, in a d- dimensional search or solution space [29]. Among all the bats, there exists a current best solution x_*. Therefore, the above three rules can be translated into the updating equations for x_i^t and velocities v_i^t:

$$f_i = f_{min} + (f_{max} - f_{min}) * \beta; \tag{9}$$
$$v_i^t = (x_i^t - x_*) * f_i; \tag{10}$$
$$x_i^t = x_i^{t-1} + v_i^t; \tag{11}$$

where $\beta \in [0, 1]$ is a random vector drawn from a uniform distribution. Here x_* is the current global best location (solution) which is located after comparing all the solutions among all the n bats. As the product $\lambda_i f_i$ is the velocity increment, it can be used either f_i (or λ_i) to adjust the velocity change while fixing the other factor λ_i (or f_i), depending on the type of the problem of interest. The choice of f_{min} and f_{max} (f_{min} = 0 and f_{max} = 100) depends on the domain size of the problem of interest. Initially, each bat is randomly assigned a frequency which is drawn uniformly from $[f_{min}, f_{max}]$. For the local search part, once a solution is selected among the current best solutions, a new solution for each bat is generated locally using random walk

$$x_{new} = x_{old} + \varepsilon A^t; \tag{12}$$

where $\varepsilon \in [-1, 1]$ is a random number, while $A^t = <A_i^t>$ is the average loudness of all the bats at this time step.

Variations of loudness and pulse rates

In order to provide an effective mechanism to control the exploration and exploitation and switch to exploitation stage when necessary, we have to vary the loudness A_i and the rate r_i of pulse emission during the iterations. Since the loudness usually decreases. Once a bat has found its prey, while the rate of pulse emission increases, the loudness can be chosen as any value of convenience, between A_{min} and A_{max}, assuming A_{min} = 0 means that a bat has just found the prey and temporarily stop emitting any sound. With these assumptions,

$$A_i^{t+1} = \alpha A_i^t; r_i^{t+1} = r_i^0[1 - \exp(-\gamma t)]; \tag{13}$$

where α and γ are constants.

The pseudo code of Bat is available in literature [30]. The tuned parameters for the Bat algorithm for the system considered are obtained by using minimization of cost function given by Eq. (1). The tuned parameters for the algorithm are n = 20; N = 15; A = 0.5; r = 0.25.

Results and analysis

Performance comparison of PI, PID, and PD–PID Cascade controller

The three areas system under study is provided with PI, PID, and PD–PID cascade controller separately and in each case controller gains are optimized simultaneously using BA. The optimum gains are as follows. The PI controller gains are K_{P1}^* = 0.09037, K_{I1}^* = 0.2200, K_{P2}^* = 0.0798, K_{I2}^* = 0.1065, K_{P3}^* = 0.0181, K_{I3}^* = 0.1762. The PID controller gains are K_{P1}^* = 0.0110, K_{I1}^* = 0.3058, K_{D1}^* = 0.0728, K_{P2}^* = 0.0103, K_{I2}^* = 0.0994, K_{D2}^* = 0.0118, K_{P3}^* = 0.0089,

K_{I3}^* = 0.1402, K_{D3}^* = 0.0054. The gains of PD–PID cascade controllers are shown in second column of Table 2. The dynamic responses for each controller are obtained and compared (Fig. 3). The settling time and the peak deviations are noted from the Fig. 3 and shown in Table 1. Critical observation of the numerical values of settling time and the peak deviations in the Table 1 as well as from Fig. 3, it is clearly seen that the responses corresponding to PD–PID cascade controller are better than both PI and PID controllers from the point of view of settling time, peak overshoot and magnitude of oscillations. The convergence of the cost curve for the Bat algorithm obtained in this optimization is shown in Fig. 4 and compared with that of CS and GA. When GA is used for optimization, a population size of 20 with 300 number of generation having mutation probability 0.06 and crossover probability 0.81 is considered. In case of CS, for the system considered are (Number of nests). n = 25, Discovery rate of alien eggs/solutions, p_a = 0.25. In both GA and CS, these values are selected based on the minimization of objective function given by Eq. (1). It is seen that the cost curve obtained with bat algorithm converges somewhat faster than the other two.

Performance comparison of PID, and PD–PID Cascade controller with Random load pattern

To justify the better performance of the proposed controller and optimization technique, a random load pattern as shown in Fig. 5(a) is applied to the control area1 and the performance of the proposed PD–PID Cascade controller under such condition is examined. Controller gains are optimized simultaneously using BA. The PI controller gains are K_{P1}^* = 0.0793, K_{I1}^* = 0.3013, K_{P2}^* = 0.2171, K_{I2}^* = 0. 6115, K_{P3}^* = 0.0451, K_{I3}^* = 0.4131. The PID controller gains are K_{P1}^* = 0.0211, K_{I1}^* = 0.3118, K_{D1}^* = 0.0767, K_{P2}^* = 0.0677, K_{I2}^* = 0.0904, K_{D2}^* = 0.0410, K_{P3}^* = 0.0109, K_{I3}^* = 0.4162, K_{D3}^* = 0.0053. The PD–PID Cascade controller gains K_{P1}^* = 0.5211, K_{P2}^* = 0.1111, K_{P3}^* = 0.3333, K_{D1}^* = 0.4125, K_{D2}^* = 0.5019, K_{D3}^* = 0.7010, K_{I11}^* = 0.3419, K_{I12}^*= 0.6001, K_{I13}^* = 0.2581, K_{P11}^* = 0.6704, K_{P12}^* = 0.3155, K_{P13}^* = 0.3233, K_{D11}^* = 0.3001, K_{D12}^* = 0.8103, K_{D13}^* = 0.2389. The dynamic responses obtained are represented in Fig. 5(b), and (c), where the performances of conventional PI and PID controllers are compared with the proposed PD–PID Cascade controller. Critical observation of the dynamic responses reveals that the responses with proposed PD–PID Cascade controller provide the better performance following random load change. Only two dynamic responses are shown in Fig. 5 to validate the statement.

Sensitivity analysis

Sensitivity analysis has been carried out to see the robustness of the optimum gains of PD–PID cascade controller (K_{Pi}^*, K_{Ii}^*, K_{Di}^*) obtained at nominal loading (50% of area capacity) conditions and nominal SLP to wide changes in system loading conditions, the magnitude of SLP, and the inertia constant, H. The loading is changed to ±25%. Similarly the SLP is changed in step of 1% and H is changed to ±25%. In each changed condition, K_{Pi}, K_{Ii}, and K_{Di} are optimized using BA and the optimum parameters are shown in Table 2. The system dynamic responses corresponding to optimum gain at each changed condition are obtained and are compared with that of changed system condition using K_{Pi}^*, K_{Ii}^*, and K_{Di}^* obtained at nominal condition (Figs. 6–13). Critical observation of the dynamic responses, it is clearly seen that the responses are more or less same and showing a good tolerance limit with respect to wide changes in system conditions and parameters. Thus, the gains of PD–PID controller obtained at nominal condition and parameter are robust and need not be reset for wide change in system conditions and parameters. Only eight numbers of responses are shown to justify the above statement.
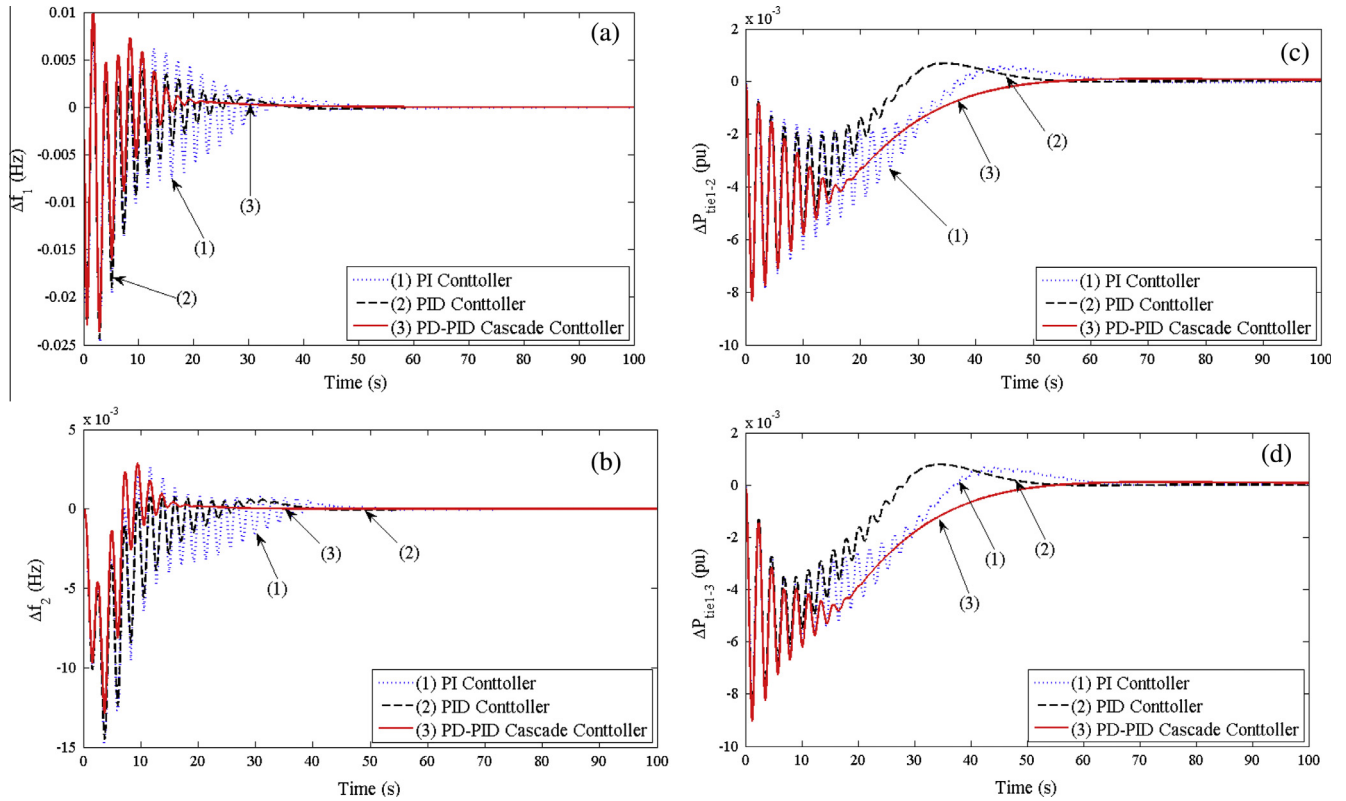
Fig. 3. Comparison of dynamic responses for different classical controllers (a) frequency deviations in Area1 vs. time, (b) frequency deviation in Area2 vs. time, (c) Tie-line power deviations in the line connecting Area1 and Area2 vs. time, (d) Tie-line power deviations in the line connecting Area1 and Area3 vs. time.

Table 1
Values of setting time, peak overshoot and peak undershoot of Fig. 3.

Fig. No.	Settling time (s)			Peak overshoot			Peak undershoot (−ve)		
	PI	PID	PD–PID Cascade	PI	PID	PD–PID Cascade	PI	PID	PD–PID Cascade
Fig. 3(a)	50.66	36.83	32.02	0.00964	0.0087	0.009	0.02467	0.0268	0.0237
Fig. 3(b)	52.01	39.71	28.34	0.00265	0.00031	0.0026	0.0014	0.0144	0.01328
Fig. 3(c)	59.08	39.07	30.13	0.0007	0.00077	0	0.00807	0.0144	0.0100
Fig. 3(d)	69.56	68.44	44.58	0.00067	0.0009	0	0.0088	0.0690	0.0081

Table 2
Optimum values of variables at different system conditions and system parameters.

Gains	Loading 50%	Loading 25%	Loading 75%	H = 3.75 s	H = 6.25 s	SLP in Area-1 2%	SLP in Area-1 3%	SLP in Area-1 4%	SLP in Area-1 5%	SLP 1 in Area-1 & 2	SLP 1 in Area-1, 2 & 3
K_{P1}^*	0.4282	0.5760	0.5300	0.3111	0.3079	0.2742	0.1102	0.4182	0.0979	0.0710	0.0670
K_{P2}^*	0.6311	0.0010	0.0010	0.5191	0.0111	0.1717	0.4777	0.2114	0.1971	0.3145	0.4640
K_{P3}^*	0.3900	0.1611	0.1466	0.4190	0.3169	0.3977	0.1004	0.5966	0.3397	0.0716	0.4375
K_{D1}^*	0.3690	0.6640	0.5325	0.2399	0.1290	0.1641	0.7231	0.4081	0.4125	0.3481	0.2126
K_{D2}^*	0.5510	0.7300	0.2610	0.7648	0.1761	0.6321	0.3794	0.5679	0.1731	0.6284	0.2175
K_{D3}^*	0.4924	0.7100	0.4897	0.2294	0.3024	0.2366	0.2218	0.0200	0.4140	0.2264	0.0156
K_{I11}^*	0.2660	0.6600	0.4411	0.6155	0.8104	0.3664	0.4000	0.6600	0.1904	0.6786	0.5775
K_{I12}^*	0.6311	0.6270	0.8900	0.3993	0.4739	0.8654	0.3979	0.8900	0.3939	0.6999	0.6129
K_{I13}^*	0.5881	0.4531	0.3190	0.4015	0.2150	0.4864	0.4811	0.3024	0.2210	0.3077	0.5458
K_{P11}^*	0.6654	0.6900	0.6590	0.2110	0.2355	0.6264	0.5921	0.6317	0.2737	0.5337	0.5790
K_{P12}^*	0.4151	0.8100	0.4275	0.5311	0. 3154	0.5852	0.7111	0.6033	0. 3224	0.2882	0.2139
K_{P13}^*	0.4855	0.6100	0.6099	0.5080	0.6079	0.3167	0.3133	0.2590	0.6010	0.7087	0.3766
K_{D11}^*	0.3308	0.0918	0.4830	0.1908	0.2898	0.6348	0.5438	0.0847	0.4898	0.7900	0.0464
K_{D12}^*	0.4734	0.1860	0.6425	0.5734	0.5011	0.4254	0.1255	0.1488	0.5051	0.4770	0.0599
K_{D13}^*	0.2000	0.7101	0.4155	0.2001	0.1999	0.14448	0.2009	0.3333	0.2047	0.2906	0.3855
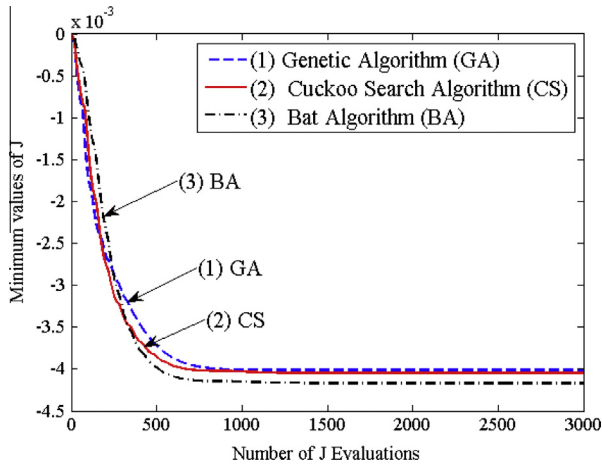
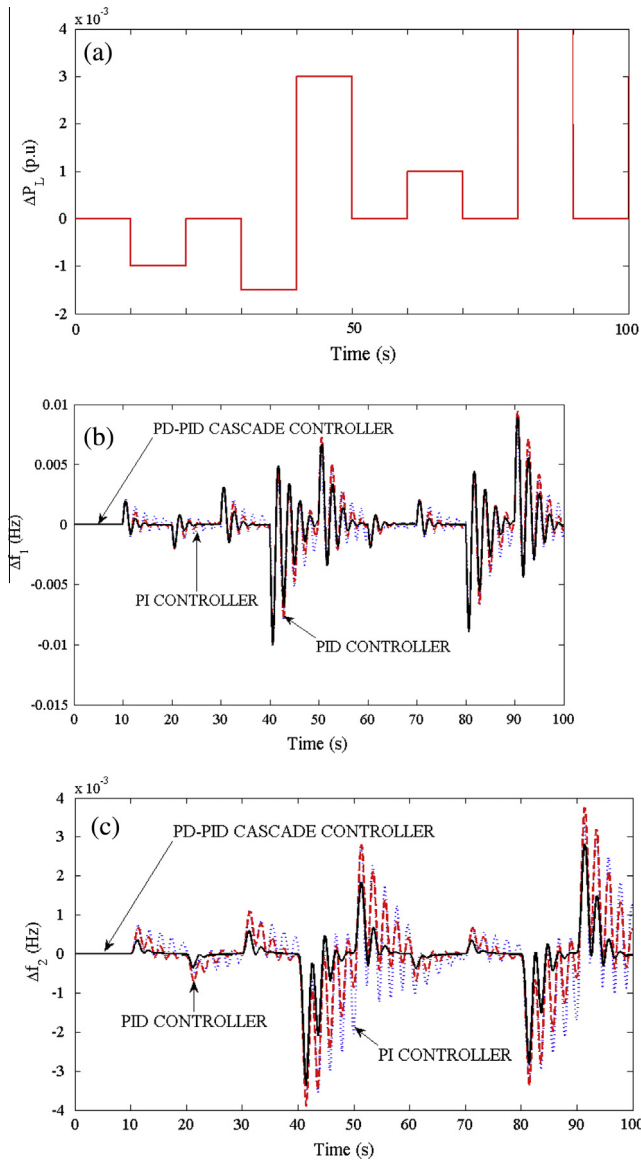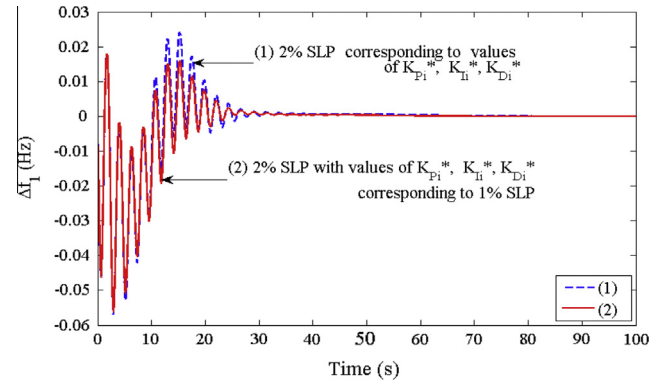Fig. 4. The convergence curves for various algorithms.

Fig. 6. Comparison of frequency deviation in Area1 vs. time for 2% SLP in Area1 with K_{Ii}^*, K_{Pi}^*, K_{Di}^* corresponding to 1% and 2% SLP in Area1.
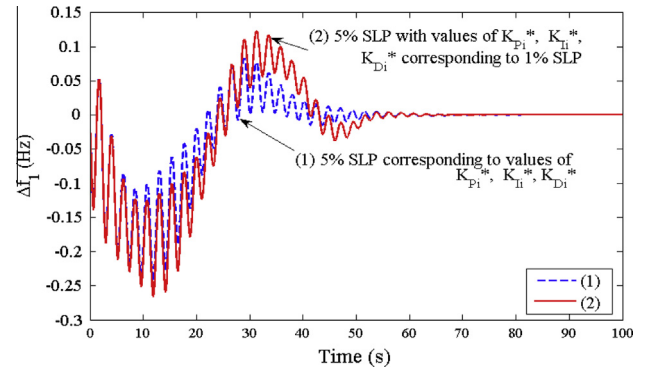

Fig. 7. Comparison of frequency deviation in Area1 vs. time for 5% SLP in Area1 with K_{Ii}^*, K_{Pi}^*, K_{Di}^* corresponding to 1% and 5% SLP in Area1.
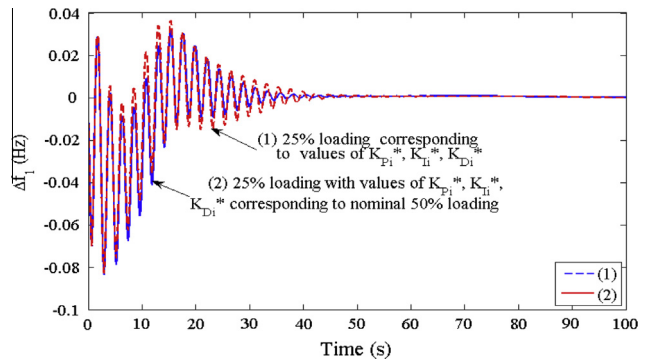

Fig. 8. Comparison of frequency deviation in Area1 vs. time for 25% loading with K_{Ii}^*, K_{Pi}^*, K_{Di}^* corresponding to 50% nominal loading and 25% loading.
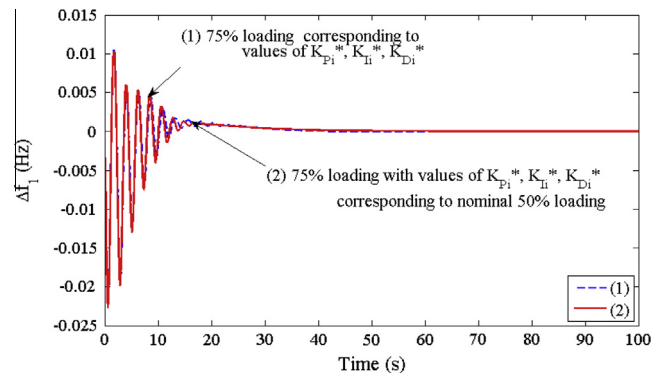
Fig. 9. Comparison of frequency deviation in Area1 vs. time for 75% loading with K_{Ii}^*, K_{Pi}^*, K_{Di}^* corresponding to 50% nominal loading and 75% loading.
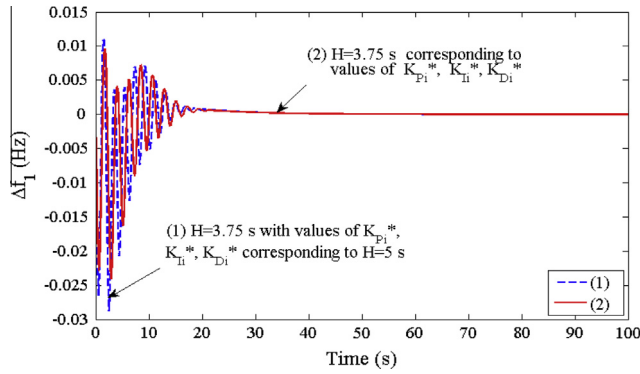
Fig. 5. (a) Random load pattern, (b) frequency deviation in Area1 obtained using PID and PD–PID Cascade controller vs. time, (c) frequency deviation in Area 2 obtained using PID and PD–PID Cascade controller vs. time.

Fig. 10. Comparison of frequency deviation in Area1 vs. time for $H = 3.75$ s with K_{Ii}^*, K_{Pi}^*, K_{Di}^* corresponding to $H = 5$ s (Nominal) and $H = 3.75$ s.
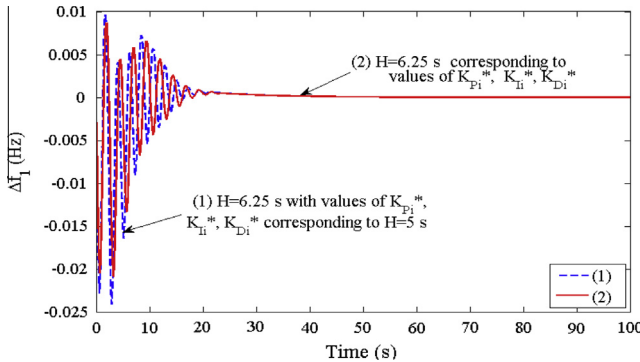

Fig. 11. Comparison of frequency deviation in Area1 vs. time for $H = 6.25$s with K_{Ii}^*, K_{Pi}^*, K_{Di}^* corresponding to $H = 5$ s (Nominal) and $H = 6.25$ s.
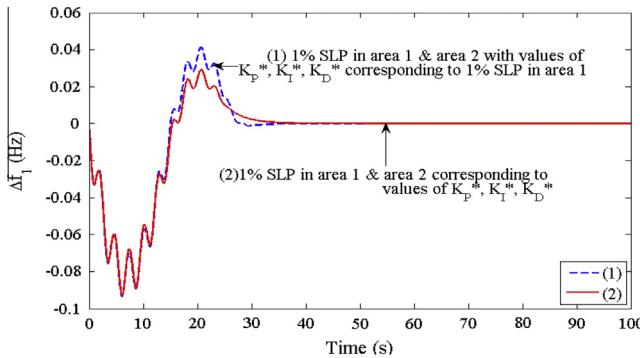

Fig. 12. Comparison of frequency deviation in area1 vs. time for 1% SLP in area 1 & area 2 simultaneously with K_{Ii}^*, K_{Pi}^*, K_{Di}^* corresponding to 1% SLP in area 1 & area 2 simultaneously and 1% SLP in area1.
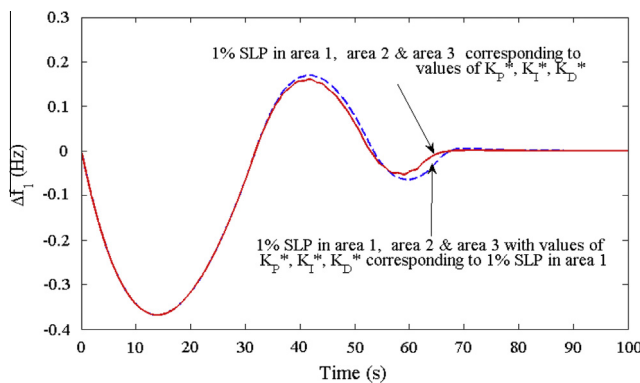

Fig. 13. Comparison of frequency deviation in Area1 vs. time for 1% SLP in area1, area2, and area3 simultaneously with K_{Ii}^*, K_{Pi}^*, K_{Di}^* corresponding to 1% SLP in area1, area2, and area3 simultaneously and 1% SLP in area1.

Conclusion

A maiden attempt has been made to apply a new powerful meta-heuristic optimization technique called Bat algorithm for optimization of several gains such as K_{Pi}, K_{Ii}, and K_{Di} of PD–PID cascade controller simultaneously. Results reveal that BA performs much better than GA and BF. An attempt has been made to apply heuristically optimized PD–PID Cascade controller for the first time in AGC. Comparison of performances of PI, PID, and PD–PID Cascade controllers reveals better dynamic performance of the later from the view point of settling time, magnitude of oscillations and peak overshoot under both considering 1% step load perturbation and random load pattern in area1. Sensitivity analysis of the optimum gains obtained at nominal conditions and parameters reveals that they are robust and need not be reset for wide change in system conditions and parameters. It is also required to mention that there is a scope for application of MPC based cascade control strategy in AGC.

Appendix A

Nominal parameter of the system are $f = 60$ Hz; $T_{gi} = 0.08$ s; $T_{ti} = 0.3$ s; $T_{ri} = 10$ s; $K_{ri} = 0.5$; $K_{pi} = 120$ Hz/pu MW; $T_{pi} = 20$ s; $T_{12} = 0.086$ pu MW/rad; $H_i = 5$ s; $D_i = 8.33 \times 10^{-3}$ pu MW/Hz; $B_i = \beta_i = 0.425$ pu MW/Hz; $R_i = 2.4$ pu Hz/MW; loading = 50%; Nominal SLP = 1%.

References

[1] Elgerd OI, Fosha C. Optimum megawatt frequency control of multi-area electric energy systems. IEEE Trans Power Appl Syst (PAS-89) 1970;4:556–63.
[2] Saikia LC, Nanda J, Mishra S. Performance comparison of several classical controllers in AGC for multi-area interconnected thermal system. Int J Electric Power Energy Syst 2011;33(3):394–401.
[3] Sahu RK, Panda S, Rout UK. DE Optimized parallel 2-DOF PID controller for load frequency control of power system with governor dead-band non-linearity. Electric Power Energy System 2013;49:19–33.
[4] Puja Dash, Saikia Lalit Chandra, Sinha Nidul. Comparison of performances of several Cuckoo search algorithm based 2DOF controllers in AGC of multi-area thermal system. Int J Electr Power Energy Syst 2014;55:429–36.
[5] Lee Yongho, Park Sunwon. PID controller tuning to obtain desired closed loop responses for cascade control systems. Ind Eng Chem Res 1998;37:1859–65.
[6] Jeng Jyh Cheng, Sinn Jia Liao. A simultaneous tuning method for cascade control systems based on direct use of plant data. Ind Eng Chem Res 2013;52:16820–31.
[7] Saikia Lalit Chandra., AGC of a three area thermal system using MLPNN controller: A preliminary study, ECTI-CON, 9th International Conference, 2012, 1–4.
[8] Chown GA, Hartman RC. Design and experience with a fuzzy logic controller for automatic generation control (AGC). Power Syst, IEEE Trans 1998;13(3):965–70.
[9] Benyo Imre, Cascade generalized predictive control-application in power plant control, Faculty of technology, department of process and environmental engineering, University of OULU, 2006.
[10] Hongbin Liu, MinJung Kim, JungJin Lim, ChangKyoo Yoo, Performance assessment of cascade control strategy in wastewater treatment process, Control Automation and Systems (ICCAS), International Conference, 2010, 696–701.
[11] Venkat Aswin N et al. Distributed MPC strategies with application to power system automatic generation control. IEEE Trans Control Syst Technol 2008;16(6):1192–206.
[12] Liu Xiangjie, Kong Xiaobing, Deng Xizhi, Power System Model Predictive Load Frequency Control, American Control Conference, Montréal, Canada, 2012, 6602–07.
[13] Kaya Ibrahim. Improving performance using cascade control and a smith predictor. ISA Trans 2001;40:223–34.
[14] Nanda J, Kothari ML, Satsangi PS. Automatic Generation Control of an interconnected hydrothermal system in continuous and discrete modes considering generation rate constraints. IEE Proc 1983;130:17–27.
[15] Oysal Yusuf. A comparative study of adaptive load frequency controller designs in a power system with dynamic neural network models. Energy Convers Manage 2005;46:2656–68.
[16] Ghoshal SP. Application of GA/GA-SA based fuzzy automatic generation control of a multi-area thermal generating system. EPSR 2004;70:115–27.
[17] Nanda J, Mishra S, Saikia Lalit Chandra. Maiden application of bacterial foraging-based optimization technique in multiarea automatic generation control. IEEE Trans Power Syst 2009;24:602–8.

[18] Yang XS. Firefly algorithm for multimodal optimization, stochastic algorithms: foundations and applications. SAGA, Lecture Notes Comput Sci 2009;5792:169–78.

[19] Saikia LC, Sahu SK. Automatic generation control of a combined cycle gas turbine plant with classical controllers using Firefly Algorithm. Electrical Power Energy Syst 2013;53:27–33.

[20] Yang X-S, Deb S. Cuckoo search via Lévy flights. In: Proceedings of World Congress on Nature & Biologically Inspired Computing. IEEE Publications, USA, 2009, 210–14.

[21] Payne RB, Sorenson MD, Klitz K. The cuckoos. New York: Oxford University Press; 2005.

[22] Tan WS, Hassan MY, Majid MS, Rahman HA. Allocation and sizing of DG using Cuckoo Search algorithm, Power and Energy (PECon), IEEE International Conference, 2012,133–38.

[23] Yildiz Ali R. Cuckoo search algorithm for the selection of optimal machining parameters in milling operations. Int J Adv Manuf Technol 2013;64:55–61.

[24] Bhandari Ashish Kumar, Singh Vineet Kumar, Kumar Anil, Singh Girish Kumar. Cuckoo search algorithm and wind driven optimization based study of satellite image segmentation for multilevel thresholding using Kapur's entropy. Expert Syst Appl 2014;41(7):3538–60.

[25] Dash Puja, Saikia Lalit Chandra, Sinha Nidul. Comparison of performances of several FACTS devices using cuckoo search algorithm optimized 2DOF controllers in multi-area AGC. Int J Electr Power Energy Syst 2015;65:316–24.

[26] Nguyen Thang Trung, Vo Dieu Ngoc, Truong Anh Viet. Cuckoo search algorithm for short-term hydrothermal scheduling. Appl Energy 2014;132:276–87.

[27] Altringham JD. Bats: biology and behavior. Oxford: Oxford University Press; 1996, 262.

[28] Gandomi Amir H, Yang XS, Alavi Amir H, Siamak Talatahari. Bat algorithm for constrained optimization tasks. Neural Comput Applic 2013;22:1239–55.

[29] Yang XS, Gandomi Amir H. Bat algorithm: a novel approach for global engineering optimization. Eng Optim Eng Comput 2012;29:464–83.

[30] Yang XS. Bat algorithm: literature review and applications. Int J Bio-Inspired Comput 2013;5:141–9.

[31] Tamiru L, Fakhruldin Hashim M. Use of fuzzy systems and bat algorithm for energy modeling in a gas turbine generator. IEEE Colloq Humanities, Sci Eng Res 2011:305–10.

[32] Khan K, Sahai A. A Comparison of BA, GA, PSO, BP and LM for training feed forward neural networks in e-learning context. I.J. Intell Syst Appl 2012;7:23–9.

[33] Johnson Michael A., Moradi Mohammad H., PID Control: New Identification and Design Methods, Springer International Edition, 2010, 103–06.

[34] Vilanova Ramon, Visioli Antonio, PID Control in the Third Millennium: Lessons Learned and New Approaches, Springer International Edition, 237–53.